CIVIL ENGINEERING JOURNAL

Article no. 13

THE CIVIL ENGINEERING JOURNAL 2-2024

RESEARCH ON CONSTRUCTION TECHNOLOGY OF LARGE-DIAMETER SHIELD TUNNEL IN SHALLOW COVER SECTION OF RED STRATA GEOLOGY

Jian Ouyang[1], Haijun Wang[1], Xin Dong[1], Dawei Hu[2], Kexin Zhang[3] and Xingwei Xue [4]

1. *Engineering Department, Guangzhou Expressway Co., LTD, Guangzhou, China*
2. *Tunnel Engineering Department, China Railway Fourth Survey and Design Institute Group Co., LTD, Wuhan, China*
3. *Shenyang Jianzhu University, School of Transportation and Surveying Engineering, Department of Bridge and Tunnel Engineering, Shenyang, China; jt_zkx@sjzu.edu.cn*
4. *Shenyang Jianzhu University, School of Transportation and Surveying Engineering, Department of Bridge and Tunnel Engineering, Shenyang, China*

ABSTRACT

This paper is based on the construction of the Haizhuwan Tunnel in Guangzhou, which passes through predominantly mudstone and sandstone red strata geology. Excavation is carried out using a slurry balance shield tunneling machine with both atmospheric pressure and pressurized cutterheads, and real-time excavation parameters recorded by the shield equipment are collected and statistically analyzed. Discovery: In the initial shallow-buried excavation section, the total thrust of the shield machine increased as the tunneling distance increased. By continuously adjusting the excavation parameters during construction, the shield machine gradually tended towards a stable operating state, leading to a gradual reduction in the range of thrust fluctuations. East Line: After excavating the reinforcement area, the increase in cutterhead torque is significant, leading to a more pronounced adaptation process for the shield machine. The cutterhead torque fluctuates more on rings 20 to 65 on the East Line, showing greater variability. This situation is related to the wear of the cutterhead and the condition of the shield machine equipment on the East Line. West Line: After excavating the reinforcement area, the cutterhead torque is initially reduced, with a slow and continuous increase in torque from rings 20 to 65, eventually stabilizing at around 12 MN·m. Throughout the excavation process, the shield machine on the East Line maintained a relatively high excavation speed within the reinforced soil at the face, with an average of 7.76 mm/min. As the machine excavated beyond the reinforcement area, the overall excavation speed of the shield machine slowed down. The excavation speed from ring 21 to ring 65 was primarily controlled between 2 to 6 mm/min, with an average of 4.49 mm/min, showing a relatively stable overall change.

KEYWORDS

Shield tunnel, Complex red strata geology, Shallow buried section, Excavation parameters, Atmospheric pressurized, Pressurized cutterhead

BACKGROUND

China's research on large diameter shield tunneling technology started later than that of foreign countries. In 1994, China introduced a large diameter shield with a diameter of Ø11.22m from

Mitsubishi Heavy Industries of Japan for the construction of the south section of the Yantai East Road tunnel in Shanghai. This model was successfully applied in Shanghai's homogeneous soft ground, laying a technical foundation for the application of large diameter shield tunnels in China [1-3]. Subsequently, by tracking the progress of shield tunneling technology overseas, China began to research the application technology of large-diameter and super-large-diameter shields in tunnel construction [4-8]. In the 21st century, driven by large-scale construction projects in the country, various models and specifications of shield tunneling machines have entered the tunnel construction field in large numbers, providing a wealth of engineering application experience and technology for the localization of shield tunneling equipment [9-12]. The Shanghai Shangzhong Road Tunnel was the first to use a super large-diameter slurry shield tunnel boring machine with a diameter of 14.87 meters. Subsequently, the Shanghai Changjiang Road Tunnel used two 15.43-meter diameter shield tunneling machines, and Nanjing Weiqi Road used two 14.96-meter diameter shield tunneling machines. This marked the successive construction of large-diameter shield tunneling projects in China, indicating the widespread application of super large-diameter shield tunneling projects in China [13]. Currently, China has become the primary market for super large-diameter shield tunneling projects in the world. In 2015, the Tuen Mun Tunnel in Hong Kong was constructed using a slurry shield tunnel boring machine with a diameter of 17.6 meters, making it the world's largest diameter shield tunnel currently in operation [14].

According to statistical analysis of construction cases, the super large-diameter shield tunneling machines used in China are mainly of European and Japanese origin, with European machines accounting for over 60%. In recent years, with the rapid advancement of domestic shield tunneling technology, domestically produced machines have fully occupied the market in new construction projects in China. In the field of super large diameter shield tunneling, domestic machines have achieved complete independent research and development, with some technologies taking a leading position [15-17]. In terms of shield tunnel types, 90% of them are slurry shield tunnels, as slurry shield tunnels have better safety and geological adaptability in coping with complex geological conditions such as high-water pressure, varying soil hardness, and developed fractures [18].

Currently, both domestic and foreign scholars have conducted extensive research on the correlation between shield tunneling process parameters and the physical properties of rock and soil. However, most of them focus on theoretical calculations and the establishment of prediction models, and statistical analysis of a large amount of measured data is not common. In addition, the shallow buried shield tunnel has the characteristics of high buried depth, and the ground movement is obvious due to the loss of the bottom layer in the construction process, which has a great impact on the surrounding environment. Therefore, higher requirements are put forward for excavation, drainage, grouting and other methods, and the construction difficulty is increased. Therefore, this article is based on the Guangzhou Haizhuwan Tunnel project. The geological conditions in this section are unique, with the shield tunneling section consisting of red strata geology, primarily composed of muddy sandstone. The 1-65 ring of shield tunneling is shallow buried section, and the construction conditions are more complicated. The Haizhuwan Tunnel is divided into east and west lines, each using different types of tunnel boring machines (TBM) - one with a constant pressure cutterhead and the other with a pressurized cutterhead. The study collects and statistically analyzes six tunneling parameters recorded in real time by the shield tunneling equipment, and investigates their patterns of change.

INTRODUCTION TO ENGINEERING BACKGROUND

This project is the Haizhuwan Tunnel project, with the main line designed from chainage EK0-415.730 to EK3+933.057, with a total length of 4348.787 m. The starting point of the main line design of this project connects to the existing Dongxiaonan Viaduct. The route extends southward and passes through the Pearl River Lijiao Waterway, Luoxi Island, and Sanzhixiang Waterway in the form of a double-tube single-layer shield tunnel. After the shield tunnel ends at the northern end of

Nanpu Road, it continues to pass through Nanpu Road in the form of a buried tunnel and emerges on the surface, connecting to the bridge of the southern section of the project.

The design adopts the planned centerline revised according to the urban planning standards. The starting point connects to the Dongxiaonan Viaduct with a dual 4-lane bridge. After crossing Nanzhou Road, it descends to the ground, and passes under the Pearl River Lijiao Waterway, Luoxi Island, and Sanzhixiang Waterway using shield tunneling. Moving southward, it goes through Nanpu Road in an underground buried tunnel, then emerges on the surface to connect to the bridge of the southern section of the project. The total length of the tunnel is 3463.057 m, with the shield tunnel section being 2077 m long and the cut-and-cover section being 1386.057 m long. The shield tunnel has an outer diameter of 14.5 m and is designed to accommodate a dual 6-lane configuration. The minimum horizontal radius for the shield tunnel section is 1000 m, while for the onshore section it is 450 m, and for the Dongxiao South Viaduct, it is 160 m. The typical minimum clearance between adjacent tunnel sections is generally not less than 1.0 times the tunnel diameter, while the clearance at the beginning and ending sections is usually controlled at around 0.6-0.7 times the tunnel diameter. The minimum spacing for the gradient change points within the tunnel is 342.467m, which meets the specified regulatory requirements. The mainline has a minimum gradient of 0.3% and a maximum longitudinal slope of 4%. The vertical curve's minimum radius for the viaduct section is 3000 m, meeting the design speed requirement of 60km/h. For the tunnel section, the minimum radius for the vertical curve is 3800 m, also meeting the design speed requirement of 60 km/h. The strata crossed by the shield tunnel section are mainly composed of strong, moderate, and slightly weathered silty sandstone. The longitudinal section layout is shown in Figure 1.

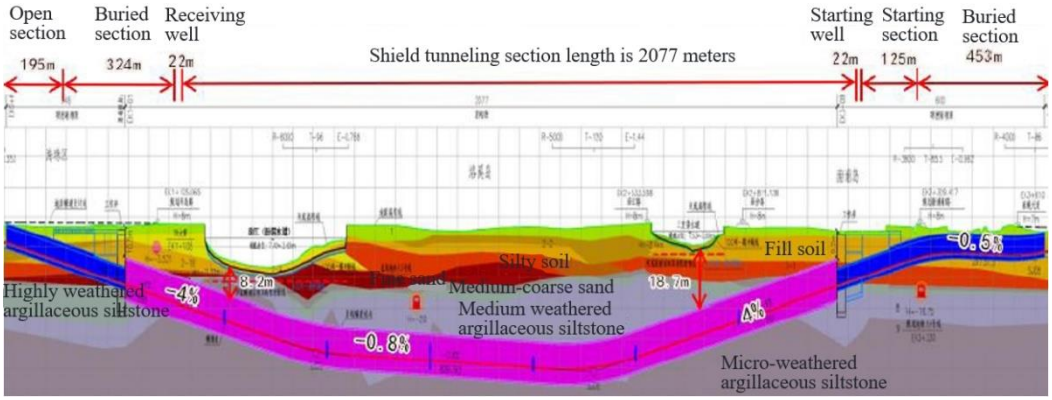

Fig. 1 – Illustration of the geological conditions in the shield tunnel section of Haizhuwan

The shield tunneling method is used for the middle section of the tunnel. The shield section has a circular cross-section with an outer diameter of 14.5 m, an inner diameter of 13.3 m, and a segment thickness of 0.6 m. The cross-sectional layout is shown in Figure 2.

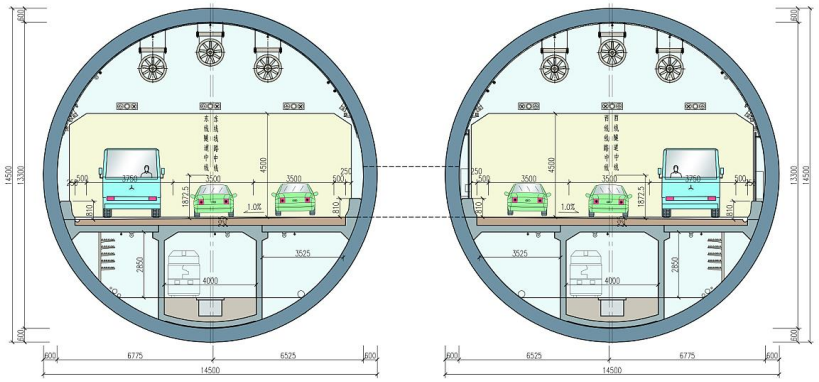

Fig. 2 – Cross-sectional diagram

OVERVIEW OF SHIELD TUNNELING MACHINE

Two slurry shield tunneling machines are used in the shield tunneling section. The excavation diameter of the shield tunneling machine is 15.07 m. The shield tunneling machine in the East line is divided into a main machine and 4 auxiliary cars behind it. The shield tunneling machine in the West line is divided into a main machine and 5 auxiliary cars behind it, with a maximum excavating speed of 50 mm/min. The technical parameters of shield machine is shown in Table 1, and the technical parameters of cutter head of shield machine is shown in Table 2.

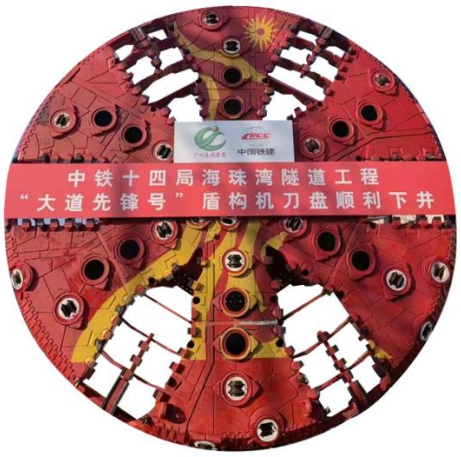

Fig. 3 – The layout diagram of the western line disc cutter (atmospheric pressure)

Fig. 4 – The layout diagram of the eastern line disc cutter (under pressure)

Tab. 1 - Technical parameters of shield machine

Herrenknecht slurry balance tunnel boring machine		China Railway Construction Heavy Industry Corporation with a mud-water balance shield tunnel boring machine	
Cutterhead diameter (m)	15.07	Cutterhead diameter (m)	15.07
Total length (m)	152	Total length (m)	128
Total weight (t)	4495	Total weight (t)	4300
Total power (kW)	11200	Total power (kW)	9755
Main drive power (kW)	5600	Main drive power (kW)	5600
Rated torque (kN.m)	42972	Rated torque (kN.m)	42784
Operating pressure (bar)	9	Total thrust (kN)	222173

Tab. 2 - Technical parameters of cutter head of shield machine

Herrenknecht slurry balance tunnel boring machine		China Railway Construction Heavy Industry Corporation with a mud-water balance shield tunnel boring machine	
Cutter opening rate (%)	30	Cutter opening rate (%)	35
Knives	246	Knives	387
Edge scraper	12	Edge scraper	16
Atmospheric pressure replaceable scraper	50	Center hob	6
Pressure replaceable center hob	12	Front hob	77
Atmospheric pressure replaceable front hob	60	Edge hob	22
Atmospheric pressure replaceable edge hob	4	Wide cutter	180
Ordinary scraper	150	Edge scraper	16
Plain side scraper	12	Over cutter	2

STRENGTHENING MEASURES AT THE DEPARTURE END HEAD

The clear dimensions of the departure work shaft pit are: length of 22 m, width of 54 m, height of 25.10 m, with a subsequent length of 126 m (114m for the east line). It has an underground four-story double-box structure and is constructed using an open-cut method in the order of excavation. The excavation support structure adopts a 1.2 m underground diaphragm wall combined with internal support bracing as the shoring scheme, and the bottom of the pit is reinforced with a skirt edge combined with struts. The starting shaft end uses Φ850 mm@ 600 triple-axis mixing piles, with a row of Φ800 mm @ 600 triple jet grouting piles for reinforcement near the working shaft. The reinforcement length is 20 m, and the reinforcement depth extends 1m below the strong weathered silty sandstone. An 800 mm thick plain wall is closely placed around the reinforcement body, extending to 5 m below the shield tunnel lining structure. The lower end reinforcement uses grouting, with the grouting range extending to the bottom of the mixing reinforcement body and 5 m below the

structure bottom. The reinforcement width extends 5 m on both sides of the structure outline, with the installation of dewatering wells. The mixing pile reinforcement of the work shaft should be completed before the excavation of the foundation pit, while the jet grouting piles should be constructed after the completion of the structural filling and before the start of the shield tunneling. As shown in Figure 5 and Figure 6.

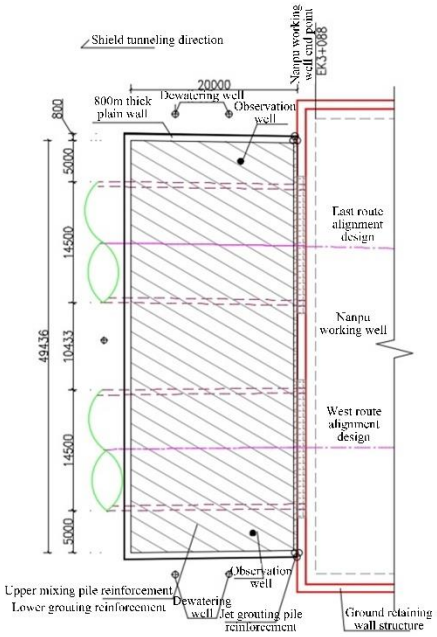

Fig. 5 – Plan view of the reinforcement at the starting shaft end

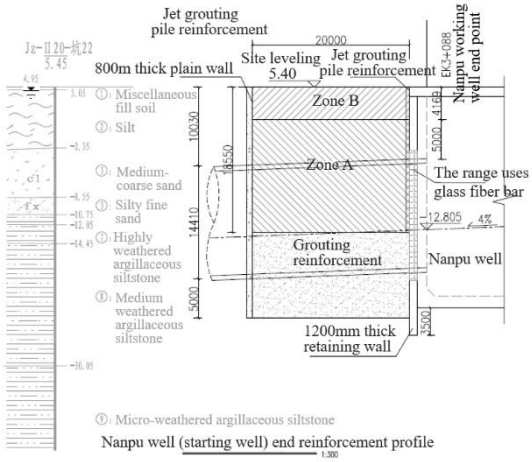

Fig. 6 – Section view of the reinforcement at the starting shaft

ANALYSIS OF THE EXCAVATION PARAMETERS IN THE SHALLOW BURIAL SECTION

Analysis of the thrust force of the tunnel boring machine

The variation curve of the thrust force of the tunnel boring machine in the process of excavating rings 1-65 in the shallow burial section can be found in Figure 7.

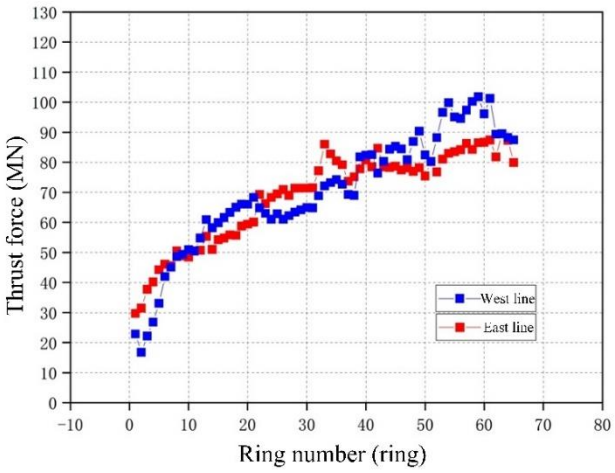

Fig. 7 – Graph of thrust variation in shallow burial section

It can be seen from Figure 7 that after the start of the tunnel boring machine on the west line, there are stage differences in the variation of thrust in the shallow burial section. During the tunnel boring process from ring 001 to ring 020, due to the stable soil in the front-end reinforcement area, the thrust force of the tunnel boring machine continues to increase to 70 MN. However, it is limited by the initial reaction frame and the stability of the cutterhead, so the thrust is controlled at a relatively low level. During the tunnel boring process from ring 021 to ring 032, as the tunnel boring machine excavates out of the front-end reinforcement area and encounters significant changes in geological conditions, the thrust force of the tunnel boring machine shows a slow decreasing trend, with an average thrust force of 64.3 MN. During the tunnel boring process from ring 033 to ring 065, as the tunnel boring machine operates at increasing depths and mainly encounters silty sandstone formations, the thrust force of the tunnel boring machine continues to steadily increase. Due to the rapid changes between soft and hard rock and soil formations in this section, the cutterhead experiences uneven loading, leading to significant eccentric loads and overturning moments on the cutterhead. When passing through the interface between soft and hard rock and soil formations, the cutterhead will experience high lateral impact loads, resulting in noticeable fluctuations in thrust force during excavation in this geological layer.

After the launch of the shield tunnel boring machine in the eastern section, the thrust force of the tunnel boring machine in the shallow-buried section overall continues to steadily increase. During the tunnel boring process from ring 001 to ring 020, the tunnel boring machine is located in the front-end soil reinforcement area, with good geological engineering properties. In the initial ten rings, the thrust force of the tunnel boring machine continuously and rapidly increases to 50 MN. In the subsequent ten rings, as the tunnel boring machine is about to excavate out of the front-end reinforcement area, the thrust force tends to increase slowly due to significant changes in geological conditions. During the tunnel boring process from ring 021 to ring 050, as the tunnel boring machine operates at increasing depths, it mainly enters silty sandstone formations. The thrust force of the tunnel boring machine continues to steadily increase. During the initial rings of tunnel boring, after the tunnel boring machine adapts to the normal soil layers, the thrust force increases from 60MN to 70 MN in stages. In the subsequent ten rings, the thrust force remains at 70 MN to ensure the stability of the tunnel boring machine excavation. The variation in thrust from rings 030 to 050 is an adaptive process for the tunnel boring machine to adjust to the new geological conditions. In the initial rings, the thrust increases from 70 MN to 86 MN in stages. However, due to the thrust not matching the geological conditions, the value gradually decreases afterwards, eventually stabilizing at 80kN. In the tunnel boring process from ring 051 to ring 065, the thrust of the tunnel boring machine continues to steadily increase. Due to rapid changes between soft and hard rock and soil formations in this section, uneven loading on the cutterhead causes the cutterhead to bear significant eccentric loads and overturning moments. When the cutterhead passes through the interface between soft and hard rock and soil, significant lateral impact loads are generated. In this geological layer, the thrust of the tunnel boring machine fluctuates significantly, with the thrust maintained at 80 to 90 MN.

In the initial shallow-buried excavation section, the total thrust of the tunnel boring machine increases with the excavation distance, and the excavation parameters are continuously adjusted during construction. The tunnel boring machine gradually reaches a stable operating state, resulting in a gradual reduction in the range of thrust fluctuations. Overall, due to the smaller curve radius on the western line, the total thrust on the western line is higher than that on the eastern line.

When the tunnel boring machine passes through the reinforcement zone at the starting end, the thrust increases rapidly due to the greater strength of the soil in the reinforced area. A comparison of the thrust variation curves between the eastern and western lines reveals that the thrust gradually increases with the increase of excavation distance, displaying a basic linear change. When excavating in the formations outside the reinforcement zone, both the eastern and western lines experience a certain degree of fluctuation in thrust, and the magnitudes of the fluctuations are essentially the same between rings 20 and 40. Subsequently, the thrust of both the eastern and western lines continues to increase. The thrust of the tunnel boring machine on the eastern line

gradually increases from 80.8 MN to 89.5 MN, while the thrust of the tunnel boring machine on the western line gradually increases from 82.41 MN to 101.83 MN. On the one hand, the thrust required for the disc cutters to crush the rock mass increases significantly with the increase in the proportion of the rock mass at the cutter face; on the other hand, in the composite soil-rock formations, the disc cutters wear out fast, leading to severe abnormal wear and a decrease in the rock-breaking ability of the cutterhead. During the excavation process in the shallow-buried section, the thrust of the cutterhead with constant pressure on the western line is between 69MN and 101.83 MN, while the thrust of the cutterhead with pressure on the eastern line is between 71 MN and 89.5 MN.

Cutterhead Torque Analysis.

The change curve of the cutterhead torque in the process of tunneling from ring 1 to ring 65 in the shallow-buried section is shown in Figure 8.

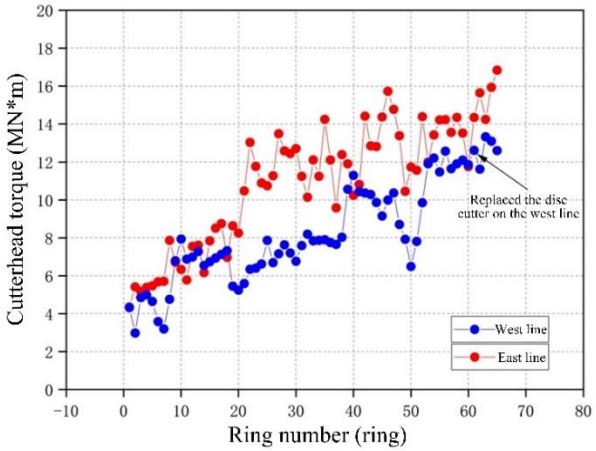

Fig. 8 – Cutterhead torque variation diagram in shallow-buried section

It can be seen from Figure 8 that the cutterhead torque of the westbound shield machine remains relatively stable overall during the tunneling process in the shallow-buried section. However, due to the limitations of the initial reaction frame and the stability of the cutting edge, the thrust is controlled at a relatively low level. During this period, the cutterhead torque frequently experiences sharp increases or decreases, with frequent fluctuations, while the distribution of the adjacent ring formations remains unchanged. This indicates significant differences in the flowability of the muck and the improvement effects in the adjacent ring chambers. During the tunneling of rings 001 to 020 of the shield tunnel, this section is for the stabilization of the end face. The soil is stable, and the cutterhead torque is continuously adjusted, fluctuating around 4 MN·m, and then steadily increasing to 7 MN·m. During the tunneling of rings 021 to 038 of the shield tunnel, as the shield machine excavates beyond the end face reinforcement zone, there is a significant change in the ground conditions, and the cutterhead torque shows a slow increasing trend. In the tunneling of rings 039 to 065 by the shield tunneling machine, as the depth of the shield machine increases, the shield machine mainly enters the mudstone and siltstone formations. The cutterhead torque continues to steadily increase. Due to the rapid changes between soft and hard rock and soil, the disc cutters bear uneven forces, resulting in significant eccentric loads and overturning moments on the cutterhead. The cutterhead torque fluctuates noticeably during tunneling in this formation.

After the start of the shield tunneling on the eastern line, there are phase differences in the overall variation of the cutterhead torque in the shallow buried section. In the tunneling of rings 001 to 020 by the shield tunneling machine, the shield machine is in the face soil reinforcement area, and the ground engineering properties are good. The cutterhead torque steadily increases to 8 MN·m in this section. In the tunneling of rings 021 to 065 by the shield tunneling machine, the shield machine continues to adjust to the new ground conditions after entering. The cutterhead torque

fluctuates noticeably during tunneling in this formation, with the cutterhead torque maintained at 10 to 16 MN·m.

In the initial shallow-buried tunneling section, as the tunneling distance increases, the tunneling parameters are continuously adjusted during construction. The cutterhead torque of the twin-shield tunneling machines is constantly fluctuating. The cutterhead torque can to some extent infer the working state of the main shaft and the wear of the tools. Overall, the cutterhead torque of the shield tunneling machine on the eastern line is higher than that of the western line.

When the shield tunneling machine passes through the initial face reinforcement area, the thrust of the twin-shield tunnels continues to increase due to the higher soil strength in the reinforcement zone. By comparing the thrust variation curves of the eastern and western lines, it can be observed that the thrust gradually increases with the tunneling distance, showing a generally linear trend. During tunneling in the strata outside the reinforcement area, both the eastern and western lines exhibit a certain degree of thrust fluctuation. Specifically, after tunneling out of the reinforcement area, the cutterhead torque of the eastern line undergoes a significant increase, leading to a more pronounced adaptation process of the shield machine. Between rings 20 and 65, the cutterhead torque of the eastern line shows greater fluctuations and more pronounced dispersion, which is correlated with the wear of the cutterhead tools and the condition of the shield machine on the eastern line. In contrast, the western line experiences an initial decrease in cutterhead torque after tunneling out of the reinforcement area, with a gradual and steady increase in torque between rings 20 and 65, ultimately stabilizing at around 12 MN·m.

Tunneling speed.

The variation curve of the tunneling speed of the west line during rings 1 to 65 of the shallow-buried section excavation process can be seen in Figure 9.

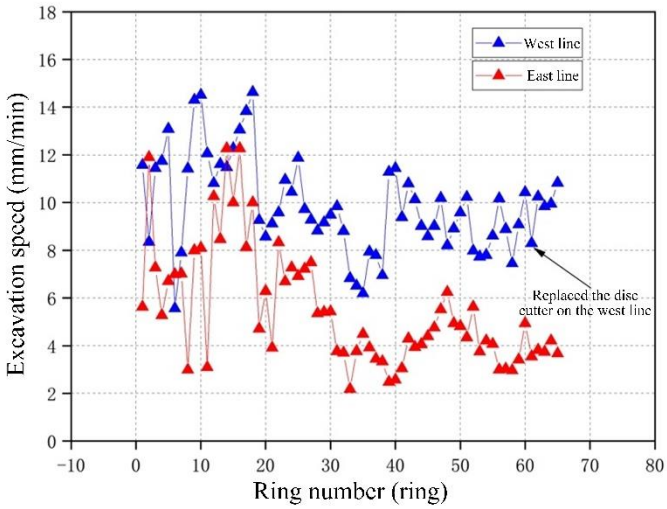

Fig. 9 – Variation of tunneling speed in the shallow-buried section

From Figure 9, it can be observed that compared to the fluctuation range of the total thrust and cutterhead torque of the west line shield machine mentioned earlier, the tunneling speed of the shield machine in the shallow-buried initial section has a higher degree of dispersion, with average and standard deviation values of 9.85 and 1.99 for the tunneling speed respectively. Throughout the entire excavation process, the tunneling speed within the face soil reinforcement area remains at a relatively high level, with an average of 11.37 mm/min. As the shield machine advances beyond the reinforcement area, the overall tunneling speed slows down, with the tunneling speed in rings 021 to 065 mainly controlled within the range of 6 to 12 mm/min, and averaging 9.18 mm/min.

Compared to the fluctuation range of the total thrust and cutterhead torque of the east line shield machine mentioned earlier, the tunneling speed of the east line shield machine shows a similar trend to the west line, with a higher degree of dispersion. The average and standard deviation of the tunneling speed are 5.49 and 2.44 respectively. Throughout the entire excavation process, the tunneling speed of the east line shield machine within the face soil reinforcement area also remains at a relatively high level, with an average of 7.76 mm/min. As the shield machine advances beyond the reinforcement area, the overall tunneling speed slows down, with the tunneling speed in rings 021 to 065 mainly controlled within the range of 2 to 6 mm/min, averaging 4.49 mm/min.

Starting from the shallow-buried starting section, the tunneling speeds of the dual-line shield machines both increase rapidly. Due to the need for the shield machine to gradually adapt to the surrounding strata in the initial stages of tunneling, the tunneling speed fluctuates greatly. As the dual-line shield machines excavate beyond the soil reinforcement area at the face, the ground conditions become more complex. Therefore, the tunneling speed of the shield machines gradually slows down and tends to stabilize with mild fluctuations. Furthermore, the shield machine has gradually adapted to the surrounding strata, so the fluctuations in tunneling speed are relatively stable. The average and standard deviation of tunneling speed for the west line are 9.85 and 1.99 respectively, while for the east line are 5.49 and 2.44. During the tunneling in the shallow-buried starting section, the tunneling speed of the east line shield machine is significantly lower than that of the west line shield machine.

Cutterhead rotation speed

The variation curve of cutterhead rotation speed for rings 1 to 65 during the tunneling process in the shallow-buried section of the west line can be seen in Figure 10.

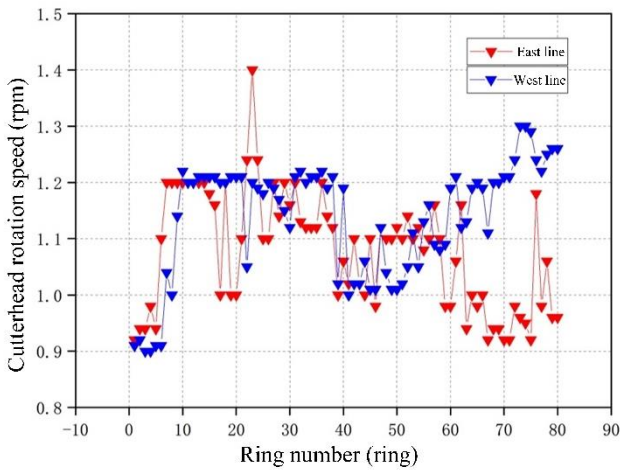

Fig. 10 – Cutterhead rotation speed variation in the shallow-buried section

From Figure 10, it can be seen that after the start of the west line shield tunneling, the rotation speed of the cutterhead continues to increase to 1.2 rpm during the excavation of the end soil reinforcement section. From rings 10 to 40, the cutterhead rotation speed is mainly maintained at around 1.2 rpm with minimal fluctuations. After ring 40, when the shield machine enters the complex strata with variations in soil hardness, in order to reduce the disturbance to the surrounding soil during excavation, the cutterhead rotation speed is reduced from 1.2 rpm to 1.0 rpm in the lower layer of this strata. As the proportion of rock mass on the cutting face increases, the rolling cutter in the complex strata wears out quickly, experiences severe abnormal wear, and the rock-breaking ability of the cutterhead decreases. The cutterhead rotation speed gradually increases to 1.2 rpm. Due to the need for constant adjustments to adapt to the strata, there is significant fluctuation in the cutterhead rotation speed during excavation in this strata.

After the start of the east line shield tunneling, the rotation speed of the cutterhead continues to increase to 1.2 rpm during the excavation of the end soil reinforcement section. From rings 10 to 30, the cutterhead rotation speed is mainly controlled at around 1.2 rpm, showing significant fluctuations. After ring 30, in order to better adapt to different strata conditions, the cutterhead rotation speed is reduced from 1.2 rpm to around 1.1 rpm. With the increasing proportion of rock mass at the face, the rolling cutter in the composite strata wears out quickly and exhibits severe abnormal wear, resulting in reduced rock breaking efficiency of the cutterhead. As a result, the cutterhead rotation speed fluctuates continuously between 0.9 and 1.2 rpm.

In the initial shallow-buried excavation section, the cutterhead rotation speed is continuously adjusted during construction as the excavation progresses. The cutterhead rotation speed fluctuates significantly between 0.9 and 1.2 rpm. The average cutterhead rotation speed for the shield machine in the west line is 1.11 rpm, while in the east line, it is 1.10 rpm. Overall, the cutterhead rotation speed in the east line shows a higher level of dispersion compared to the west line.

Cutting water pressure and air bubble chamber pressure

The variation curves of cutting water pressure and air bubble chamber pressure in the excavation process of rings 1-65 in the shallow-buried section of the west line can be seen in Figure 11.

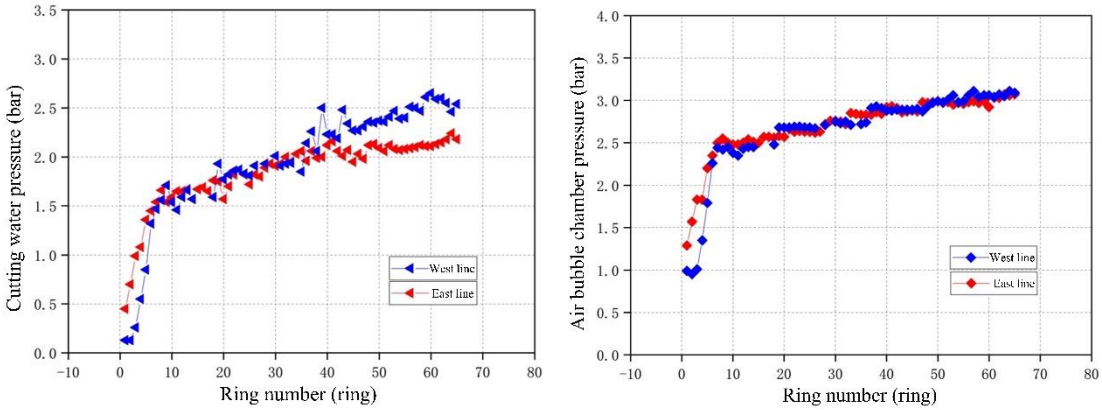

(a) Cutting water pressure *(b) Air bubble chamber pressure*

Fig. 11 – Cutterhead rotation speed variation in the shallow-buried section

According to Figure 11, it can be seen that with the continuous increase of the excavation distance of the west line shield tunnel, the tunnel depth also increases accordingly. Therefore, the cutting water pressure and ai bubble chamber pressurer bubble chamber pressure of the shallow-buried starting section of the west line shield tunnel both show an overall increasing trend. During the excavation of rings 001 to 010 of the shield tunnel, due to being in the end soil reinforcement zone, the cutting water pressure and air bubble chamber pressure of the west line shield tunnel both increased rapidly. The cutting water pressure increased from 0.13 bar to 1.54 bar, and the air bubble chamber pressure increased from 0.99 bar to 2.38 bar. In the subsequent rings 011 to 065, the cutting water pressure and air bubble chamber pressure continued to increase, but compared to the first ten rings, the rate of increase slowed down, with smaller fluctuations and a more stable trend.

The cutting water pressure and air bubble chamber pressure of the shallow-buried starting section of the east line shield tunnel follow the same pattern as the data for the west line tunnel, with both values gradually increasing. During the excavation of rings 001 to 010 of the shield tunnel, the cutting water pressure and air bubble chamber pressure of the east line shield tunnel both increased rapidly. The cutting water pressure increased from 0.45 bar to 1.59 bar, and the air bubble chamber pressure increased from 1.29 bar to 2.48 bar. In the subsequent rings 011 to 065, the cutting water

pressure and air bubble chamber pressure continued to increase, but compared to the first ten rings, the rate of increase slowed down.

The cutting water pressure and air bubble chamber pressure of the shallow-buried starting section of the east and west lines both show a gradually increasing trend. The standard deviations of the cutting water pressure in the shallow-buried starting section of the east and west lines are 0.34 and 0.6, respectively, indicating that the west line cutting water pressure has a higher degree of dispersion compared to the east line cutting water pressure; the standard deviations of the air bubble chamber pressure in the shallow-buried starting section of the east and west lines are 0.34 and 0.50, respectively, indicating that the west line air bubble chamber pressure has a higher degree of dispersion compared to the east line air bubble chamber pressure.

Grouting volume

The curve showing the changes in the grouting volume of the west tunnel boring machine in rings 1 to 65 of the shallow-buried section is shown in Figure 12.

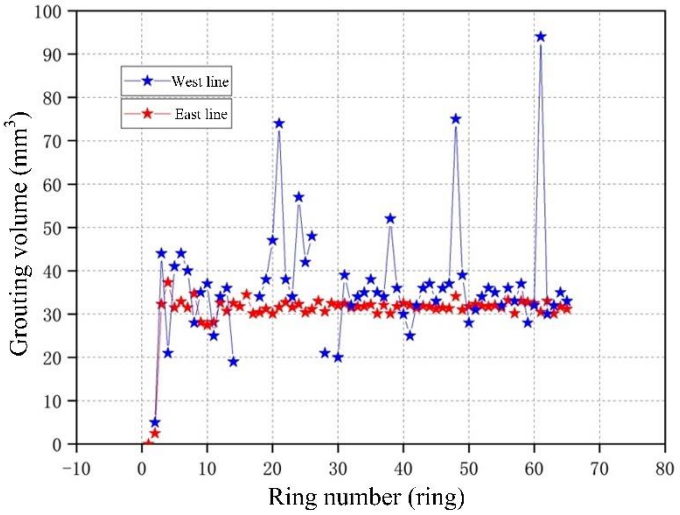

Fig. 12 – C Graph of grouting volume changes in the shallow-buried section

As can be seen from Figure 12, the average grouting volume of the west tunnel boring machine is 36.66 m^3, showing a trend of fluctuation around the average throughout the entire excavation process of the shallow-buried starting section. The average grouting volume of the east tunnel boring machine is 30.76 m^3. Throughout the entire excavation process of the shallow-buried starting section, except for the initial 3 rings, the grouting volume at the remaining segment lining rings remains relatively stable.

The grouting volumes of the east and west tunnel boring machines in the shallow-buried starting section remained within specific values, with fluctuations in the data corresponding to different ring numbers. The standard deviations of the grouting volumes for the east and west tunnel boring machines in the shallow-buried starting section are 5.50 and 13.21 respectively, indicating that the grouting volume of the west tunnel boring machine has a higher level of dispersion compared to the east tunnel boring machine.

ANALYSIS OF GROUND SURFACE SETTLEMENT MONITORING SECTION RESULTS

The ground surface settlement caused by shield tunnel excavation is essentially the cumulative soil loss caused by shield tunnel construction. In order to study the dynamic process of ground surface settlement during shield tunnel construction, five transverse monitoring sections, DB1 (0 m

from the starting shaft), DB2 (20 m from the starting shaft), DB3 (40 m from the starting shaft), DB4 (60 m from the starting shaft), and DB5 (80 m from the starting shaft), were selected as target surfaces. The dynamic relationship curves between ground surface settlement and the excavation face advancement process are shown in Figures 13 to 17.

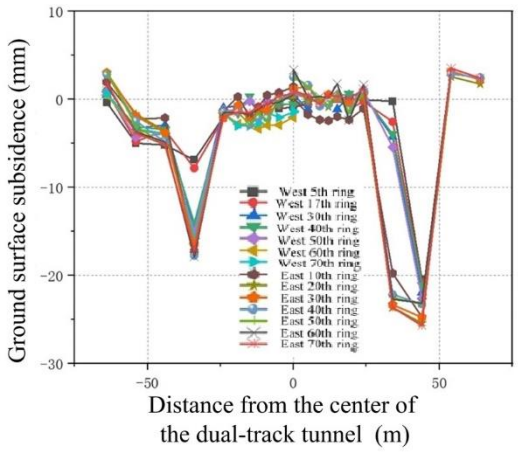

Fig. 13 – Settlement curve of transverse monitoring section DB1

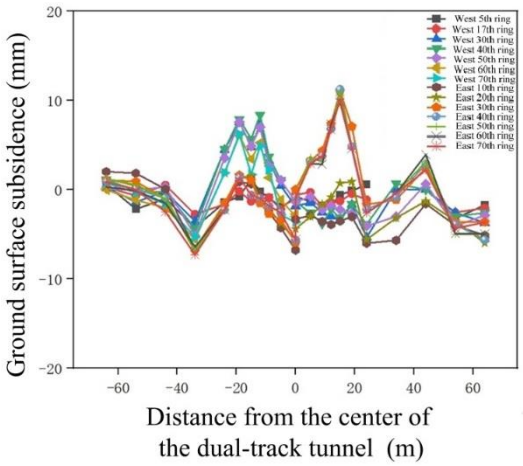

Fig. 14 – Settlement curve of transverse monitoring section DB

From Figure 13 and Figure 14, it can be seen that before the shield tunneling machine reaches the section, there is no significant ground settlement. With the excavation of the west line (leading tunnel) and the east line (following tunnel) shield tunnels, as the transverse monitoring sections DB1 (0 m away from the originating shaft) and DB2 (20 m away from the originating shaft) are both located within the initial section head reinforcement zone, reinforcement measures such as bored piles ensure the formation of cement soil in the reinforcement zone, with good engineering properties. No significant ground settlement occurred near the axis of the twin tunnels and the excavation sections, indicating the reasonable and effective implementation of the measures taken, ensuring the safe progress of the originating construction. After the shield tunneling machine of the east line tunnel passes through, significant settlement occurred at the edge of the originating shaft and the head reinforcement zone due to the apparent difference in soil properties. The maximum settlement on the west side of section DB1 is about 18 mm, and on the east side is about 26 mm, the maximum settlement on the west side of section DB2 is about 7 mm, and on the east side is about 6 mm.

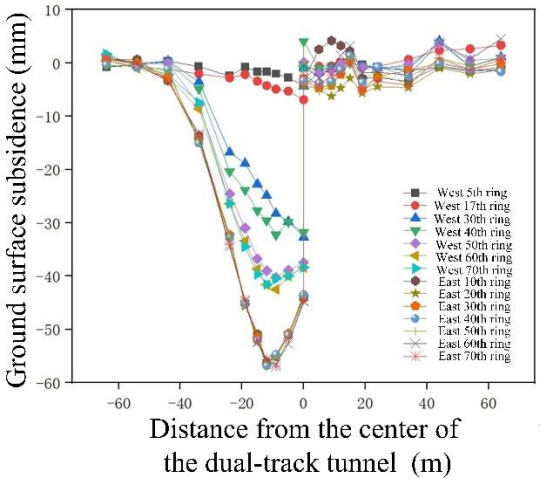

Fig. 15 – Shows the settlement curve of transverse monitoring section DB3.

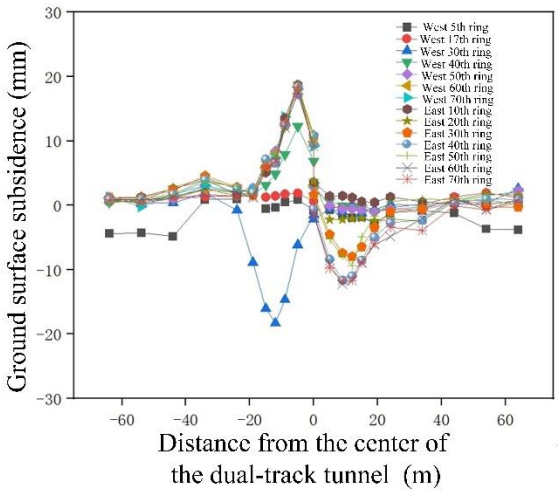

Fig. 16 – Shows the settlement curve of transverse monitoring section DB4.

From Figure 15, it can be seen that with the excavation of the shield tunnel of the west line (leading tunnel), there is no significant settlement on the ground surface before the shield tunnel machine of the west line arrives at the section. After the DB3 section (40 m from the starting shaft), surface settlement gradually occurs. When the tunnel machine reaches Ring 20, it crosses the monitoring section DB3. At this point, the surface settlement of the DB3 section significantly increases, and the settlement values and settlement rates at the tunnel axis are noticeably greater than those on both sides of the tunnel. As the shield tunnel machine of the west line crosses the section, the settlement curve develops into a normal distribution curve. The single-line excavation of the west line tunnel conforms to the settlement law of the Peck theory. The maximum transverse surface settlement value of 42.51 mm is obtained at the axis of the west line tunnel, with a settlement trough width of approximately 44m, conforming to the settlement trough theory. This indicates that tunnel excavation will cause lateral differential settlement on the ground surface.

With the excavation of the shield tunnel of the east line (trailing tunnel), monitoring data shows that before the shield tunnel machine arrives at the section, there is approximately 4.18 mm of ground uplift at the axis of the east line tunnel section. As the construction progresses, when excavating to Ring 20, the shield tunnel machine crosses the monitoring section, and the surface settlement of the DB3 section significantly increases. The surface settlement values and settlement rates at the tunnel axis are noticeably greater than those on both sides of the tunnel. At this point, the maximum transverse surface settlement value of 6.24 mm is obtained at the axis of the east line tunnel, with a settlement trough width of approximately 15 m. As the shield tunnel machine of the east line crosses the section, after the grouting is completed, the strata slowly undergo consolidation and rheology, eventually reaching a new stress equilibrium, and the ground surface stabilizes. Due to the disturbance of the surrounding soil caused by the excavation of the west line tunnel, the surface settlement values overlap with those generated during the excavation of the east line tunnel. The position of the maximum settlement point shifts towards the centerline of the two tunnels, ultimately reaching a maximum settlement value of 56.96 mm. The width of the settlement trough continues to increase, and the final shape remains V-shaped.

Based on the results of the engineering geological exploration, it is believed that before the shield tunnel machine reaches the monitoring section DB3, the settlement is mainly caused by consolidation of the overlying soft soil layer. When the shield tunnel machine crosses the section until grouting is completed at the tail of the shield, shear stress is generated at the interface between the shield and the soil, as the diameter of the shield tunnel machine is slightly larger than the outer diameter of the tunnel lining, and simultaneous grouting cannot instantly fill the gap between the

tunnel lining and the soil. The surrounding soil rapidly moves towards the gap, leading to a rapid occurrence of surface settlement, which can be considered as instantaneous settlement. After grouting is completed, the strata slowly undergo consolidation and rheology, eventually reaching a new stress equilibrium, and the ground surface stabilizes. It can be seen that significant surface settlement occurs during the shield tunnel crossing the section and before grouting is completed at the shield tail.

From Figure 16, it can be seen that as the shield tunnel of the west line (leading tunnel) is excavated, there is no significant surface settlement before the shield tunnel machine of the west line reaches the section. Subsequently, surface settlement gradually occurs at the DB4 section (60 m from the starting well). When excavation reaches ring 30, the shield tunnel machine crosses the monitoring section, and surface settlement at the DB3 section significantly increases. The maximum lateral surface settlement value at the axis of the west line tunnel is 18.31 mm, with a settlement trough width of approximately 34 m. The surface settlement value and settlement rate at the tunnel centerline are significantly greater than those on both sides of the tunnel. As the shield tunnel machine of the west line crosses the section, the area near the west line tunnel gradually transitions from settlement to uplift. The maximum lateral surface uplift value within the west line tunnel is 18.07 mm.

As the shield tunnel of the east line (trailing tunnel) is excavated, the monitoring data shows that there is approximately 1.23 mm of ground uplift at the axis of the east line tunnel before the shield machine reaches the section. When excavating to ring 30, the shield tunnel machine crosses the monitoring section, and surface settlement at the DB4 section significantly increases. The surface settlement value and settlement rate at the tunnel centerline are significantly greater than those on both sides of the tunnel. At this time, the lateral surface settlement value at the axis of the east line tunnel is 7.95 mm. As the shield tunnel machine of the east line crosses the section, after the grouting is completed, the strata slowly undergo consolidation and rheological changes, eventually reaching a new stress equilibrium, and the ground surface stabilizes. Due to the disturbance caused by the excavation of the west line tunnel, the surface settlement values generated during the excavation of the east line tunnel are superimposed. The position of the maximum settlement point shifts towards the centerline between the two tunnels, resulting in a maximum settlement value of 12.24 mm. The settlement trough shows a V-shaped pattern.

Compared to the previous three sections, in the lateral monitoring process of this section, there is a significant ground uplift near the axis of the west line tunnel. Based on the results of engineering geological exploration and grouting volume data in the shallow buried section (see Figure 12), it is believed that the main cause of surface settlement is the drastic fluctuation in grouting volume during the excavation of the west line tunnel. From Figure 12, it can be seen that the grouting volume for the west line tunnel from ring 29 to ring 30 is 20m3 each, while the average grouting volume for the west line shield tunnel is 36.66 m^3, indicating a significant undersupply of grouting volume. When the west line tunnel advances to ring 31 to ring 35, significant surface settlement has occurred. It is reasonable to increase the control of grouting at this point. However, due to insufficient grouting in the earlier rings, a sudden increase in grouting volume at this stage causes the strata to quickly undergo rheological changes, leading to surface uplift. The grouting volume for the west line tunnel shows a significantly higher level of dispersion compared to the grouting volume for the east line tunnel, indicating that the control of surface settlement during the excavation of the east line tunnel is clearly better than that of the west line tunnel. It can be seen that it is highly important to make reasonable adjustments and controls to excavation parameters during shield tunneling.

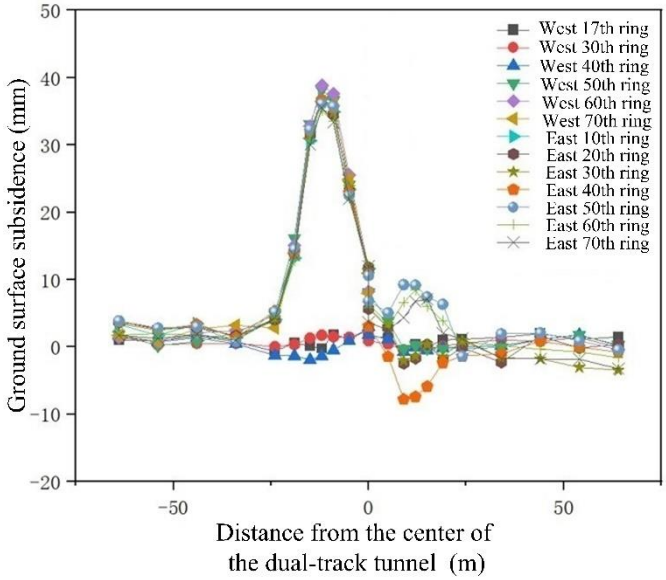

Fig. 17 – Shows the settlement curve of transverse monitoring section DB4.

From Figure 17, it can be seen that as the excavation of the west line (leading tunnel) shield tunnel progresses, monitoring data before the arrival of the shield machine at the section of the west line tunnel axis shows that a ground uplift of approximately 1.73 mm occurs at the west line tunnel axis. When excavating through ring 40, the shield machine crosses the monitoring section. The surface settlement of DB3 section significantly increases, with the maximum lateral surface settlement value obtained at the west tunnel axis reaching 1.94 mm. The settlement trough width is approximately 34 m, and the surface settlement value and settlement rate at the tunnel axis are significantly greater than those on both sides of the tunnel. As the shield machine of the west line tunnels through the section, the area near the west line tunnel gradually changes from settlement to uplift. The maximum lateral surface uplift value of 38.85 mm is achieved on the inside of the west line tunnel.

As the shield tunnel of the east line (trailing tunnel) is excavated, there is no apparent surface settlement before the shield machine reaches the section. When excavating to ring 40, the shield machine crosses the monitoring section, and the surface settlement of the DB5 section significantly increases. Due to the disturbance of the surrounding soil caused by the excavation of the west line tunnel, the surface settlement values generated during the excavation of the east line tunnel are superimposed. The position of the maximum settlement point shifts towards the centerline of the two tunnels. At this point, the maximum lateral surface settlement value of 7.8 mm is obtained at the inner measuring point of the east line tunnel axis. As the shield machine of the east line tunnels through the section, after grouting is completed, the strata slowly undergo consolidation and rheological changes, eventually reaching a new stress equilibrium, and the surface stabilizes. The maximum settlement value eventually reaches 3.37mm, and the settlement trough appears in a V shape.

Similar to section DB4, during the lateral monitoring process of the measuring points in this section, there is also a noticeable surface uplift near the axis of the west line tunnel. This is mainly caused by improper adjustment of the grouting volume in the excavation parameters. The grouting volume of the west line is relatively more dispersed compared to that of the east line. In this section, the advantage of the east line tunnel in controlling surface settlement throughout the excavation process is more evident, further confirming the importance of properly adjusting and controlling excavation parameters.

CONCLUSION

(1) In the initial shallow-buried excavation section, as the excavation distance increases, the total thrust of the shield machine is continuously adjusted during construction. The shield machine gradually reaches a stable operational state, resulting in a gradual reduction in the fluctuation range of the thrust values. Overall, due to the smaller curve radius of the west line, its total thrust is higher than that of the east line.

(2) After the excavation and reinforcement zone on the east line, the cutterhead torque experiences significant growth, leading to a more noticeable adaptation process for the shield machine. The fluctuation of the cutterhead torque is greater in rings 20 to 65 on the east line, showing higher levels of dispersion. This situation is correlated with the wear of the cutterhead and the condition of the shield machine equipment on the east line. On the west line, after the excavation and reinforcement zone, the cutterhead torque is initially decreased. From ring 20 to ring 65, the torque gradually and slowly increases, eventually stabilizing around 12 MN·m.

(3) The excavation speed of the shield machine on the east line displays a similar trend to that on the west line, with a higher level of dispersion. The average and standard deviation of the excavation speed are 5.49 and 2.44, respectively. During the entire excavation process, the shield machine on the east line maintains a relatively high excavation speed within the end soil reinforcement zone, with an average of 7.76 mm/min. As the excavation progresses beyond the reinforcement zone, the overall excavation speed of the shield machine slows down. In rings 021 to 065, the excavation speed is mainly controlled between 2 to 6 mm/min, with an average of 4.49 mm/min. Overall, the speed changes more steadily.

(4) In the initial shallow excavation section, the cutterhead speed is continuously adjusted during construction as the excavation progresses. The cutterhead speed fluctuates noticeably between 0.9 to 1.2 rpm. The average cutterhead speed for the shield machine on the west line is 1.11 rpm, while the average cutterhead speed for the shield machine on the east line is 1.10 rpm. Generally, the cutterhead speed on the east line has a higher level of dispersion compared to the west line.

(5) The water pressure at the cutting face and the air bubble chamber pressure in the initial shallow excavation sections of the east and west lines are showing a gradually increasing trend. The standard deviations of the water pressure at the cutting face in the initial shallow excavation sections of the east and west lines are 0.34 and 0.6, respectively, indicating that the water pressure at the cutting face on the west line has a higher level of dispersion compared to the east line. Similarly, the standard deviations of the air bubble chamber pressure in the initial shallow excavation sections of the east and west lines are 0.34 and 0.50, respectively, indicating that the air bubble chamber pressure on the west line has a higher level of dispersion compared to the east line.

REFERENCES

[1] Gou, Yuxuan, et al, “Experimental study on the mechanical response of metro shield tunnels obliquely crossing ground fissures”, Tunnelling and Underground Space Technology, vol. 132, pp. 104849, 2023, doi: 10.1016/j.tust.2022.104849

[2] Yi, Haiyang, et al, “Influence of long-term dynamic load induced by high-speed trains on the accumulative deformation of shallow buried tunnel linings”, Tunnelling and Underground Space Technology, vol. 84, pp. 166-176, 2019, doi: 10.1016/j.tust.2018.11.005

[3] Li, Chenyang, et al, “Deformation and failure analysis of metro shield tunnel induced by active ground fissure in Xi'an, China”, Engineering Failure Analysis, vol. 142, pp. 106776, 2022, doi: 10.1016/j.engfailanal.2022.106776

[4] Zhao, Mingji, et al, “Optimization of Construction Parameters and Deformation Characteristics of Large-Section Loess Tunnel: A Case Study from Xi’an Metro”, Advances in Civil Engineering vol. 2021, pp.1-21, 2021, doi: 10.1155/2021/6639089

[5] Guo, Kai, and Limao Zhang, “Multi-source information fusion for safety risk assessment in underground tunnels”, Knowledge-Based Systems, vol. 227, pp. 107210, 2021, doi: 10.1016/j.knosys.2021.107210

[6] Lu, Yao, et al, “Deformation characteristics and internal force analysis of shield hoisting construction of working shaft in silty clay strata: Case study in Jinan”, IOP Conference Series: Earth and Environmental Science, vol. 570, no. 5, 2020, doi: 10.1088/1755-1315/570/5/052044

[7] He, Siyue, et al, “A literature review on properties and applications of grouts for shield tunnel”, Construction and Building Materials, vol. 239, pp. 117782, 2020, doi: 10.1016/j.conbuildmat.2019.117782

[8] Chen, Ren-peng, et al, “Experimental study on face instability of shield tunnel in sand”, Tunnelling and Underground Space Technology, vol. 33, pp. 12-21, 2013, doi: 10.1016/j.tust.2012.08.001

[9] Jin, Dalong, et al, “Analysis of the settlement of an existing tunnel induced by shield tunneling underneath”, Tunnelling and Underground Space Technology, vol.81, pp. 209-220, 2018, doi: 10.1016/j.tust.2018.06.035

[10] Xue, Yadong, and Yicheng Li, “A fast detection method via region‐based fully convolutional neural networks for shield tunnel lining defects”, Computer‐Aided Civil and Infrastructure Engineering, vol.33, no.8, pp. 638-654, 2018, doi: 10.1111/mice.12367

[11] Liang, Rongzhu, et al, “Simplified method for evaluating shield tunnel deformation due to adjacent excavation”, Tunnelling and Underground Space Technology, vol.71, pp.94-105, 2018, doi: 10.1016/j.tust.2017.08.010

[12] Yin, Minglun, et al, “Effect of the excavation clearance of an under-crossing shield tunnel on existing shield tunnels”, Tunnelling and Underground Space Technology, vol.78, pp.245-258, 2018, doi: 10.1016/j.tust.2018.04.034

[13] Gong, Chenjie, et al, “Waterproof performance of sealing gasket in shield tunnel: A review”, Applied Sciences, vol. 12, no.9, pp.4556, 2022, doi: 10.3390/app12094556

[14] Huang, Hong-wei, Qing-tong Li, and Dong-ming Zhang, “Deep learning based image recognition for crack and leakage defects of metro shield tunnel”, Tunnelling and underground space technology, vol.77, pp.166-176, 2018, doi: 10.1016/j.tust.2018.04.002

[15] Liu, Dejun, et al, “Structural responses and treatments of shield tunnel due to leakage: A case study”, Tunnelling and Underground Space Technology, vol.103, pp.103471, 2020, doi: 10.1016/j.tust.2020.103471

[16] Zhang, Fengshou, Xiongyao Xie, and Hongwei Huang, “Application of ground penetrating radar in grouting evaluation for shield tunnel construction”, Tunnelling and Underground Space Technology, vol.25, no.2, pp.99-107, 2010, doi: 10.1016/j.tust.2009.09.006

[17] Zhang, J., and Qi, Y, “Research on the intelligent positioning method of tunnel excavation face”, Archives of Civil Engineering, vol. LXVIII, no.1, pp.431-441, 2022, doi: 10.24425/ace.2022.140178

[18] An, H., Song, Y., and Yang, D, “Experimental study of the effect of rock blasting with various cutting forms for tunnel excavation using physical model tests” Archives of Civil Engineering, vol.67, no.3, 2022, doi: 10.24425/ace.2022.140178